Search for a local effect in multiatom resonant core excitation in a surface species: Photoemission and photon-stimulated desorption from N_2 on Ni(111)

P. Feulner, M. Ecker, P. Jakob, R. Romberg, R. Weimar, and D. Menzel*
Physik-Department E 20, Technische Universität München, D-85747 Garching, Germany

A. Föhlisch and W. Wurth
Institut f. Exp.physik, Universität Hamburg, Luruper Chaussee 149, D-22761 Hamburg, Germany

S.-H. Yang† and C. S. Fadley
Materials Sciences Division, Lawrence Berkeley National Laboratory, Berkeley, California 94720, USA and Department of Physics, University of California Davis, Davis, California 95616, USA

R. Larciprete and S. Lizzit
Elettra, Synchrotrone Trieste, Basovizza, Italy

K. L. Kostov and G. Tyuliev
Institute f. Inorg. and General Chemistry, Bulgarian Academy of Sciences, Sofia, Bulgaria
(Received 13 July 2004; published 16 March 2005)

We have investigated photoabsorption, N 1*s* photoelectron emission, and photon-stimulated desorption (PSD) of N^+ ions, from N_2 molecules perpendicularly chemisorbed on Ni(111) surfaces, in the energy range of the Ni $2p_{3/2,1/2}$ excitations. For this system, N 1*s* photoemission monitors single-core-hole production, whereas PSD of N^+ is mainly due to excitation of multiply excited N 1*s* core-hole states. The amplitude variations of these two signals and the kinetic energy distributions (KED's) of the N^+ ions were recorded as functions of the photon energy. In addition, we measured the amplitude variations of PE and PSD as a function of the photon incidence angle, which was varied from grazing (7° with respect to the surface) to steeper angles (43° and 50° with respect to the surface). For grazing incidence, strong variations of both the photoelectron and the N^+ signals with photon energy and angle of incidence were found in the Ni 2*p* region which are compatible with x-ray optical (dielectric) effects, one manifestation of multiatom resonant photoemission. The N^+ KED's, which are known to depend strongly on the nature of the electronic excitation responsible, did not change across the Ni $2p_{3/2}$ threshold, which excludes any type of state selectivity in the interatomic core-coupling effects observed. For N 1*s* photoemission, a first analysis of our data suggests a variation of the N 1*s* signal at the Ni 2*p* edges also for steeper angles of light incidence, of comparable magnitude to that at grazing incidence. However, more careful x-ray photoelectron spectroscopy experiments and the investigation of electronically stimulated desorption of neutral N_2 molecules and N atoms reveal that these effects are due to a strong increase of beam damage when passing the Ni 2*p* edge; these effects could be reduced by rapidly scanning the sample under the beam. We thus conclude that for high angles of incidence most of the Ni 2*p*-related changes in our N 1*s* photoemission signal are due to beam damage.

DOI: 10.1103/PhysRevB.71.125409 PACS number(s): 78.70.−g, 78.68.+m, 79.60.−i, 79.20.La

I. INTRODUCTION

Resonant coupling phenomena in the vicinity of electronic excitation thresholds have become an indispensable tool for the investigation of electronic interactions in matter. When the same final excited state can be reached either directly or via a discrete resonance, the interference of these paths leads to distinct features in the observed cross sections.[1] The effect is well understood for core excitations of single atoms, in which the coupling is intraatomic. The resonant behavior is experimentally observed by monitoring the photon energy-dependent cross sections directly by photoemission (PE) or indirectly by decay phenomena (decay electrons, fluorescence photons, or stimulated ion or atom emission) across the photon energy corresponding to the resonance energy. For example, valence electron photoemission in resonance with core-level excitation to a discrete level is one particularly illustrative example.[1] The resulting resonance shapes have been successfully represented by Fano profiles, the appropriate form for two interfering quantum-mechanical emission channels: one nonresonant and one resonant.[2,3] For systems consisting of more than one kind of atom, such processes are commonly described as *intra-atomic* processes; by contrast, prior work suggests that *interatomic* core-level coupling and decay via the Auger process[4] should be very weak because of the small expected wave function overlap. Nonetheless, the Coulomb interaction responsible for such effects decays relatively slowly with distance, so one can ask whether such interatomic effects should be seen in photoemission. Recently, in fact, strong effects of such coupling have been reported in heteronuclear solids (e.g., with two atoms *A* and *B*), for which the photo-

emission cross section of atom *A* is affected by crossing a core-level x-ray absorption resonance of atom *B*; these effects have been termed *multiatom resonant photoemission* (MARPE).[5–11]

Attempts by various groups to measure these effects led initially to varying conclusions, but by now a consistent picture for photoemission from bulk solids has emerged. As detected via the photoemission channel, MARPE effects were originally observed in MnO, Fe_2O_3, and $La_{0.7}Sr_{0.3}MnO_3$ (Refs. 5–8) as strong resonant enhancements that very closely followed the associated x-ray absorption coefficients; however, it was subsequently realized that these experiments on bulk samples had suffered from detector nonlinearities which dominated the apparent MARPE effects and distorted their shapes.[9–11] Some of the first conclusions concerning the magnitudes and potential utility of these effects were thus not correct. Experimental results for MnO with accurate detector nonlinearity correction have been published,[9] and the observed interatomic resonant effects have been described in terms of both a microscopic quantum-mechanical theoretical picture and a more empirical resonant x-ray optical or dielectric model.[7,9] Similar early experiments on bulk $MnCl_2, CrCl_2, VCl_2$, and KCl showed enhancements of the Cl 2*p* photoelectrons between 29% ($MnCl_2$) and 11% (KCl) for metal 2*p* excitation,[12] but these also appear to have been affected by the same detector nonlinearities.[9] Prompted by early MARPE measurements on an adsorbate system $N_2/Ni(100)$,[13] these limitations on the quantitative analysis of MARPE were identified in a systematic investigation of the detector nonlinearities for chemisorbed O/Ni(100),[14] reducing the uncorrected O 1*s*–Ni L_3 MARPE resonance of 140% to less than $2\% \pm 5\%$ for angles of x-ray incidence higher than 20°. Bulk NiO and CuO have also been studied,[15] and for these cases the O 1*s* photoemission from NiO did not show *any* modulation at the Ni $2p_{2,3}$ thresholds, whereas that from CuO showed a decreased intensity or "antiresonance" at the Cu 2*p* edge. A microscopic theory of the effect in CuO involving resonant x-ray scattering (a close relative of the x-ray optical approach) correctly predicted the observed profile[15] and is in qualitative agreement with the results for MnO.[9] A very recent detailed reinvestigation of NiO at more grazing incidence angles has also concluded that such effects can indeed be observed for this case and that the observed modulations can be explained by the resonant x-ray optical (dielectric) model, with the earlier nonobservation of any effects being due to the steep incidence angle used.[11,16]

MARPE experiments based on core-hole *decay* measurements (e.g., soft x-ray or Auger electron emission) have also provided mixed conclusions. Large enhancements (by 90%–100%) were reported for O 1*s* soft x rays and Auger electrons at the metal 2*p* edges in MnO and Fe_2O_3, respectively,[17] but these have also subsequently been attributed to detector nonlinearities in measuring the x-ray absorption coefficient.[9,11] For soft x-ray emission from LaF_3 and $Ti_xNb_{1-x}C$, no enhancement of the F and C $K\alpha$ fluorescence was seen for resonant La $M_{4,5}$ and Ti $L_{2,3}$ excitations, respectively, but rather only effects explainable via x-ray optics.[18] However, we note that such x-ray optical effects are in fact manifestations of the same set of phenomena that have been used to explain the variation of photoemission intensities with photon energy[9,11] and are as such MARPE effects as viewed by another detection mode.

For complete clarity, we also note that the x-ray optical model implies that the effects of scanning through a resonance alter the excitation step by changing the orientation and strength of the electric field in the near-surface region that is active in electron excitation. If we average over radiation polarization effects, the excitation strength will be proportional to the square of the electric field strength times a photoabsorption cross section for a given process, even though the cross section must in its most precise form be calculated as the square of the matrix element for a given polarization.

In what follows, we ask which interatomic resonant effects are observable in photoexcitation of an adsorbate, via photoelectron and desorbed ion detection. In particular we explore whether effects are present that go beyond those describable via resonant x-ray optical theory. However, we should quickly note that, since the x-ray optical constants are determined by the collective effects of all excitation processes occurring at a given photon energy, it is only via very specific short-range local-field or overlap effects, perhaps specific to the surface region, that MARPE effects may be different from those predicted by x-ray optical theory. A key experimental complication in observing such distinct short-range interatomic core-hole coupling, aside from (and aggravating) the aforementioned possible detector nonlinearities, is the strong variation of the optical constants across the absorption resonance of atom *B*, which changes the ratio of transmitted to reflected photon flux, the phase of the x-ray wave at the surface, and its penetration depth.[7,9,11] These effects, which in fact represent an integration over long-range and short-range effects, can be understood in terms of a dielectric theory of x-ray optics. The distinction and separation of short-range interatomic core-hole coupling from these at-first-sight-simpler dielectric effects requires a detailed understanding of the dielectric properties of the samples under resonant excitation, as well as very careful measurements. Considerable effort has been devoted recently to the successful development of codes for classical dielectric theory as well as of a more refined microscopic theory of such core-hole coupling.[7,9,11] We have here made use of only the dielectric theory in analyzing our data, but hope that our results stimulate future analysis via a more revealing microscopic quantum-mechanical approach.

Improvement in our understanding of these effects and of their differentiation requires experimental data for simple systems which minimize the influences of electron transport and x-ray penetration. Such a system is a well-ordered monolayer of an adsorbate acting as excitation site *A*, on a single-crystal substrate consisting of resonating atoms *B*. We have chosen N_2 chemisorbed in a vertical orientation and in a well-ordered $(\sqrt{3}\times\sqrt{3})$ superstructure on Ni(111),[19] since this layer is well defined and because the presence of two inequivalent N atoms should provide further length-scale information on any local coupling effect. For clearest exclusion of detector peculiarities we observed the resonant behavior in *two* channels: N 1*s* PE and photon-stimulated desorption (PSD) of N^+ ions, at grazing and nongrazing in-

cidence angles. The intensity of photoemission monitors the N 1*s* (single) core-hole cross section at different angles of incidence. From prior work, one expects to suppress contributions from dielectric x-ray optical effects in photoemission measurements at steeper (that is, nongrazing) angles of incidence.[9,16] PSD of N^+ ions from molecularly chemisorbed nitrogen in the N 1*s* region is by contrast very weak following single-core excitations; it is mainly brought about by overlapping bound and continuum multielectron excitations of the nitrogen molecule which set in several tens of eV beyond the [N 1*s*] edge.[20] Furthermore, previous PSD work[20] has shown an enhancement of the PSD yield of N^+ ions from N_2 on the Ru(001) surface at the Ru 3*p* thresholds, which are energetically degenerate with those multiple N 1*s* excitations and possibly could couple with them. Because of slight differences in energy positions and peak shapes seen in photoabsorption on the one hand and N^+ PSD on the other, we had tentatively explained our finding in terms of short-range MARPE involving the Ru 3*p* resonances in Ru surface atoms and the N 1*s*-derived continuum states of the N_2 molecule.[20] PSD of ions is of particular interest for the detection of MARPE because the background signal is negligible and influences of detector nonlinearities do not exist, indicating that PSD has the potential to monitor interatomic core-hole coupling with a minimum of extraneous disturbances. The understanding of effects of *total* photodesorption (leading predominantly to the neutral desorption products, N_2 molecules and N atoms), on the other hand, is—as will be shown—nonetheless important if one is to fully exclude spurious effects caused by radiation damage, and this is also true in the PE measurements.

An even clearer case than N_2/Ru for detecting distinct short-range MARPE effects beyond the dielectric x-ray optical description appears to be N_2 adsorbed on Ni(111). This adsorbate system is well characterized and understood, and the Ni $2p_{3/2,1/2}$ threshold resonances are very strong. In this study, we therefore investigated N 1*s* photoemission and N^+ ion desorption from this system at grazing and steep angles of light incidence, in the photon energy range 835—870 eV crossing the Ni $2p_{3/2,1/2}$ edges. For better characterization of the PSD ion signal and its origin, we also measured the kinetic energy distributions (KED's) of the N^+ ions at various photon energies, which are indicative of the shapes of the potential energy curves of the excited states leading to desorption and therefore vary strongly if different excited states are responsible for ion emission.[21,22] When effects of radiation damage became obvious in our PE results, we also investigated the desorption of N_2 molecules in the same range (as stressed, neutral desorption is the main signal accompanying the photoinduced destruction of the adsorbate layer).

II. EXPERIMENT

The experiments were performed at beamlines BW3 at HASYLAB/Hamburg (N^+-PSD and N 1*s* PE), UE56-PGM (KEDs of N^+ PSD) and U41-PGM (N 1*s* PE and PSD of neutrals) at BESSY/Berlin, and SuperESCA at ELETTRA/Trieste (N 1*s* PE). N_2 was adsorbed onto the clean (111) surface of an approximately 5-nm-thick Ni film epitaxially grown on a Ru(001) substrate[23] for the grazing incidence (7° to the surface, A_z polarization) measurements done in Hamburg and Berlin and for all experiments done in Trieste (50° to the surface). For the steeper incidence done in Berlin (43° to the surface), the N_2 layer was adsorbed on a Ni(111) single crystal. To obtain perfect ordering of the adlayer and a maximum amount of the perpendicularly chemisorbed N_2, the nitrogen was dosed while cooling the samples from 150 to less than 50 K. Subsequent heating to 78 K removed physisorbed N_2, leaving perpendicularly chemisorbed N_2/Ni(111),[19] as corroborated by polarization-dependent x-ray absorption spectra (XAS) of the bound N 1*s* resonance. At all beamlines, detector nonlinearities in photoemission were no problem because they were operated more than a factor of 10 away from the onset of saturation and the detectors utilized exhibit none of the low-count-rate quadratic nonlinearity which affected some prior MARPE experiments.[5,7,10,12] XAS were monitored with partial electron yield (PEY, at HASYLAB and BESSY) as well as with total electron yield (TEY, at BESSY and ELETTRA). The PSD ion yield, which poses no detector problems because of its weakness, was measured with a quadrupole mass spectrometer (HASYLAB) and with a time-of-flight detector (BESSY; see below). When the influence of beam damage became obvious, we scanned the sample mechanically through the beam so as to continuously expose new surface. A time-of-flight detector was also used to record kinetic energies of the desorbing ions[21] in single-bunch beamtime (UE56-PGM, BESSY) with one consequence being a sufficiently small photon flux that no beam damage occurred under these conditions. The yields of desorbing N_2 molecules and N atoms were measured with a different quadrupole detector which possesses a high efficiency ionization chamber in a cryopumping surrounding; apparatus and procedures have been described before in detail.[24]

III. RESULTS AND INTERPRETATION

In Fig. 1, N 1*s* PE spectra measured with photon energies varying across the Ni $2p_{3/2}$ photoabsorption threshold under grazing light incidence (7° to the surface, so essentially *z* polarization if *z* is along the surface normal) are shown. The spectra have been normalized to the incident photon flux measured with a gold photodiode. The spectra were shifted to obtain identical pre-peak levels. Each XPS spectrum shows a higher-kinetic-energy doublet due to the two chemically inequivalent inner and outer nitrogen atoms, separated by a chemical shift of 1.3 eV. This doublet is accompanied by a strong many-electron satellite structure towards lower kinetic energies. In agreement with previous MARPE-related measurements on N_2/Ni(100),[13] we observe no significant variation of the shape of the N 1*s* spectral function for the different photon energies; the intensity ratio between the two N 1*s* PE signals is constant within experimental uncertainty. However, the total N 1*s* intensity as derived from the area enclosed in the background-subtracted spectra varies significantly as a function of photon energy in the range of the Ni $2p_{3/2}$ edge, exhibiting a distinct minimum at around a kinetic energy of 447.3 eV. Qualitatively similar results were ob-

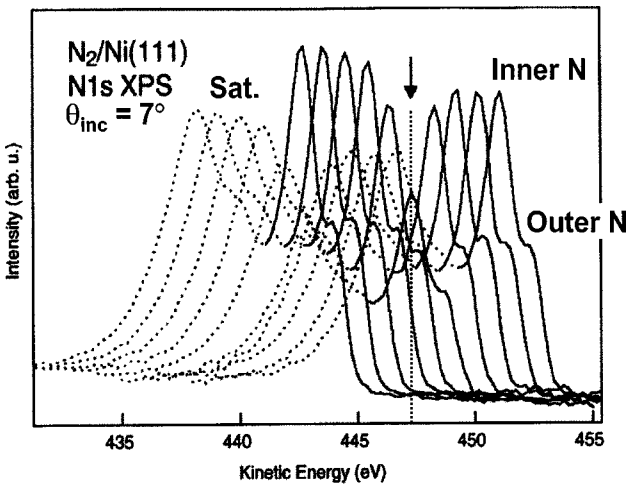

FIG. 1. N 1*s* PE spectra of N_2/Ni(111) for photon energies varying across the Ni $2p_{3/2}$ edge (arrow), measured with grazing light incidence (7° to the surface, predominantly *z* =normal polarization). The XPS main lines of the two chemically shifted N atoms are shown as solid lines; shake-up/screening satellite features as dashed lines.

tained on scanning through the Ni $2p_{1/2}$ edge, but here with a less dramatic change in intensity. The same conditions were used for measurement of the N^+ ion PSD yield.

Figure 2 combines the results of different measurements and summarizes the N 1*s* PE, the N^+ PSD, and Ni 2*p* XAS results (as measured via PEY). The scale here is with respect to the Ni $2p_{3/2}$ absorption peak located at 852.5. PE measurements are shown for two different angles of photon incidence. At grazing incidence (7° with respect to the surface) dips of about 43% and 34% of the prethreshold intensity are observed at the Ni $2p_{3/2}$ edge for the N 1*s* and the N^+ signals, respectively. The PE and PSD signals (both obtained at DESY, with the same setup) differ somewhat in shape: the minimum of the PSD signal is shifted to lower energy from that of the PE trace by 0.3 eV, and its leading edge is less steep. Both PE and PSD profiles could be well fitted by Fano

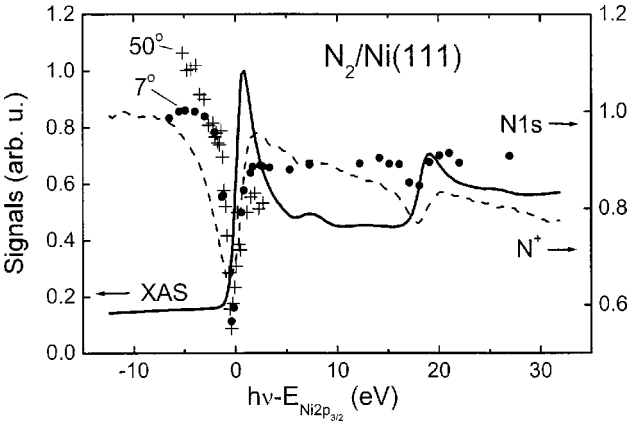

FIG. 2. Photoabsorption (XAS, solid line; grazing incidence), N^+ PSD (dashed line; grazing incidence), and N 1*s* photoemission in the Ni $2p_{3/2}$ region (7° grazing photon incidence: solid circles; nongrazing at 50°: crosses). Photon energy $h\nu$ relative to the Ni $2p_{3/2}$ edge at 852.3 eV; *z* polarization).

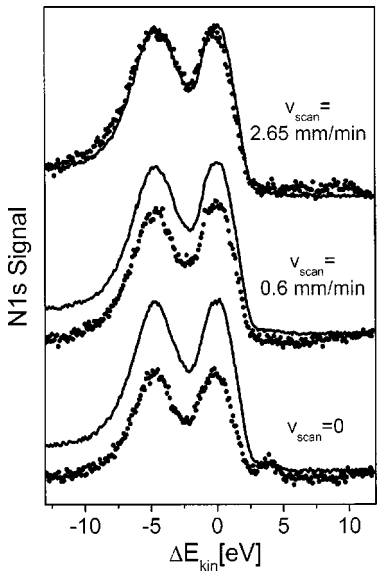

FIG. 3. Dependence of the PE signal (at low resolution for fast energy scanning) on the velocity of moving the synchrotron light beam over the surface, at a steep angle of incidence (43°). For each velocity, the line represents the measurement for an energy below the Ni resonance and the points that on resonance. Their difference is then an indication of the removal of adsorbate. The strong influence of beam damage is obvious.

line shapes, but we stress that this is a purely empirical fit of this function to the data. We emphasize that for grazing incidence, the PSD data have been recorded simultaneously with the XAS measurement, thus eliminating any differential energy calibration errors. At the Ni $2p_{1/2}$ edge the PE and PSD signals differ much less, but since the effects are smaller, resolving differences is more difficult.

Figure 2 also contains the first PE results obtained at ELETTRA using a steep angle of incidence (50° to the surface). As seen, the raw data showed a clear dip at the $2p_{3/2}$ edge, quite similar to the results for an angle of 7°. So a first possible conclusion is that there exist MARPE effects beyond dielectric x-ray optics since no appreciable effect at steep angles is expected from this mechanism, as we will illustrate later with theoretical calculations. However, the steeply falling background across the $2p_{3/2}$ region for 50° incidence—in contrast to the 7° case—already indicates the likelihood of contributions from a coverage decrease—i.e., beam damage—of the N_2 layer in this case. Local beam damage is in general expected to appear as an energy-dependent signal decrease which can be significantly enhanced on passing through an absorption resonance. Thus, such effects can mimic the behavior of a negative cross section variation by MARPE. Indeed, when we scanned the beam over the surface with varying speed, we found a strongly varying decrease of PE signal strength with scanning velocity. Figure 3 shows these data, which were taken at BESSY at an angle of incidence of 43°. The solid line is the N 1*s* spectrum off resonance, which is compared in each case to a spectrum at a different scanning rate. For the fastest scanning rate shown of 2.7 mm/min, which amounts to shifting the beam by its diameter about every 2 s, the two

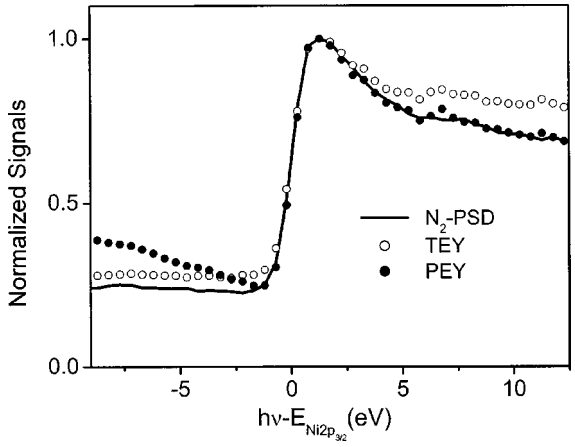

FIG. 4. XAS signals (TEY: total electron yield open circles; PEY: partial electron yield, cutoff at a maximum kinetic energy of 350 eV, solid circles) compared to the signal from desorbing neutral N_2 molecules, at the Ni $2p_{3/2}$ edge. Data obtained with grazing light incidence and *z* polarization.

sets of data are essentially in agreement, but for anything slower than this, the effect of desorption is evident. These decreases of signal are due to a proportional decrease in the local N_2 coverage seen by the beam. We also find that almost all of the removed molecules appear in the gas phase as neutral molecules. As displayed in Fig. 4, the N_2 PSD yield follows closely the TEY curve, especially as photon energy passes directly over the Ni $2p_{3/2}$ edge. This shows that the main mechanism for desorption of neutral molecules and, since this is by far the strongest channel, also of adsorbate coverage depletion, is XESD (x-ray induced electron stimulated desorption) by outgoing photo-, Auger, and secondary electrons.

It is clear, then, that, if the sample is physically scanned through the beam during measurement, but under conditions for which the radiation-induced decrease of coverage (which is directly determined by the damage cross section) changes strongly with energy, the signal will trace the inverted desorption cross section. From our data, we conclude that most (ca. 95%) of the apparent MARPE effects seen at steep angles of incidence in the PE signal are due to this radiation-induced decrease of coverage during measurement. Due to the combined uncertainties in both the raw data on and off resonance (cf. Fig. 3) and the resulting difference signal, we cannot exclude the existence of a small true MARPE effect on the PE signal over the Ni 2*p* edges for steep angles of incidence, as seen recently, e.g., at such higher angles in O 1*s* emission from bulk NiO.[11,16] For the grazing-angle measurements, we estimate that about half the raw effect seen is caused by beam damage and the other half is a true cross-section response.

As pointed out above, the N^+ ion yields should not be influenced by these depletion effects, as they were taken at much smaller light intensities. Figure 5(a) shows results for a number of angles close to grazing light (light polarization along the *z* direction) and Fig. 5(b) one curve for steep incidence. These curves depend strongly on incidence angle, and for the grazing angles, we find a strong suppression of the N^+

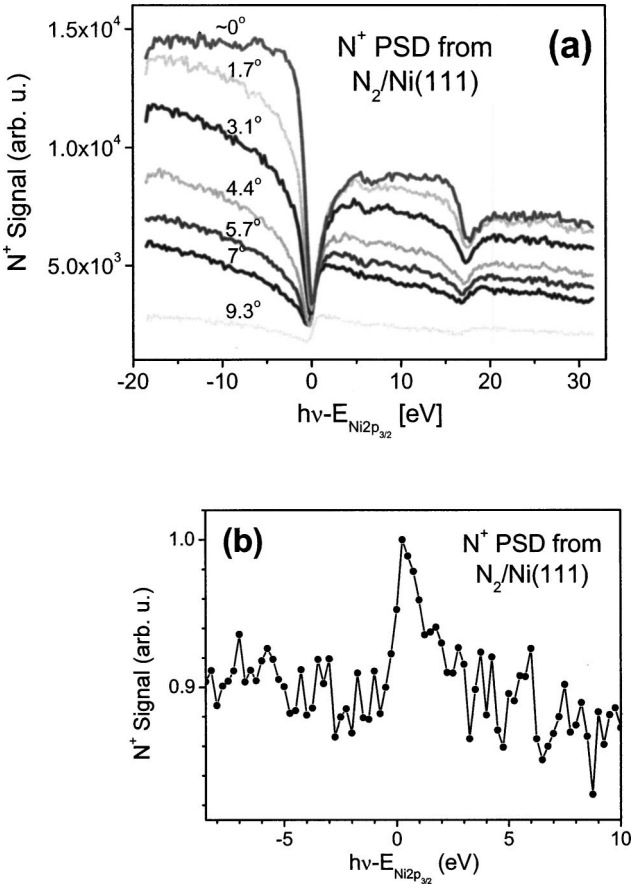

FIG. 5. N^+ PSD at the Ni $2p_{3/2}$ edge for a number of light incidence angles close to grazing (a) and at a steep angle (43°) (b). The strongly angle-dependent Fano-type curves at grazing and the small, absorptionlike response at the steep angle are clearly seen. Note the strong background suppression in (b) which shows the very small degree of enhancement of only about 10%.

signal at both Ni 2*p* resonances, with a form for the lowest angles that resembles the inverse of the absorption coefficient and for higher angles around 7°–9° more resembles decreasing-then-increasing Fano-type profiles. This general behavior is also expected from dielectric theory.[9,11,16] At the steep angle shown in the lower panel, however, only a small peak mimicking the direct XAS curve occurs on a large background. The steep-angle response can be explained essentially by XESD. A small Fano-type response could be hidden below it, but again we estimate that its strength could be at most 5% of the overall effect.

We have also measured the ion KED's at various photon energies in the same range for grazing incidence (see Fig. 6). It can be seen that the normalized curves lie exactly on top of each other. It is well established for O^+ PSD from CO/Ru(001) (Refs. 21 and 22) that the KED's change strongly when the excited state causing the ion desorption changes; very similar results have been obtained for N^+ PSD from chemisorbed N_2.[25] Thus we conclude from this constancy of the KED's that, if a MARPE effect is responsible for the intensity variations seen in PE and N^+ desorption, this effect is *not* state selective. Below the N 1*s* multiple shake-up / shake-off region (about 420 eV) the ion signal is

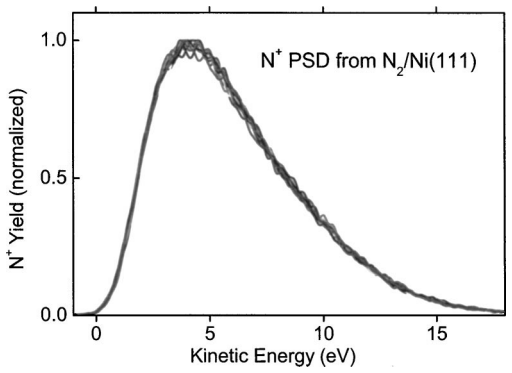

FIG. 6. Kinetic energy distributions (KED's) of N^+ ions at a number of photon energies in the Ni $2p_{3/2}$ range, normalized at the maximum. Their equality is obvious.

very small. Also, in the case of N^+ PSD from Ru (Ref. 25) the KED's measured with photon energies above 800 eV—i.e., in a range where there are *no* core thresholds—were very similar to those found here, which corroborates the molecular origin of those ions. Therefore, strong contributions from XESD via valence excitations or one hole N 1*s* ionization of the N_2 molecule by outgoing electrons can be excluded for the N^+ channel, in agreement with the small effect shown by the 50° N^+ curve of Fig. 5.

IV. DISCUSSION AND COMPARISON TO DIELECTRIC MODEL CALCULATIONS

We have already concluded from our results that (a) a true response of the N 1*s*-related signals at the Ni 2*p* thresholds occurs only at grazing angles; the effects seen at steep light incidence are due to beam damage (PE) and XESD (N^+ ions); (b) there is no discernible difference in the PE effect for the two different N atoms; (c) there is no change of the N^+ KEDs across the Ni 2*p* thresholds which means that there is no change in the dissociative final state in this range; this is most easily explained if the effect is due to x-ray optics at grazing, with a small contribution of XESD at steep incidence angles.

We nevertheless examine the overall situation from a broader perspective to make sure that all important factors have been considered.

In principle our findings could contain possible contributions from three different mechanisms:[9] (i) the variation of the effective photon field at the surface due to the dielectric response of the sample, which is equivalent to a longer-range dielectric x-ray optical effect, (ii) a shorter-range interatomic core-hole coupling and decay between the N 1*s* and the Ni 2*p* core levels that must be treated by going beyond the dielectric picture and into a microscopic theory, and (iii) photon energy-dependent photoelectron diffraction. We note that item (ii) could consist of local-field influences which might be accessible in a more detailed x-ray optical treatment and which could have their origins in local orbital overlap effects. Of course, a high-level theory would contain all three of these contributions, and the separation of the first two contributions might be considered as similar to the conceptual separation of extrinsic and intrinsic coupled excitations (with or without their cross terms) in core electron emission. We do believe, however, that such a conceptual separation between long-range and short-range contributions—if it is possible—would contribute more to a detailed understanding than a complete theory without differentiation.

Item (iii), photoelectron diffraction, can be excluded as the explanation of the observed abrupt changes (dips) at the Ni $2p_{3/2}$ edges, because at a kinetic energy of the photoelectrons exceeding 400 eV, photon-energy-dependent variations due to diffraction are very gradual on a scale of a few eV; also, they would be accompanied by an intensity variation between the N 1*s* photoemission of the two inequivalent N atoms, which is not observed.

As noted in the introduction, the effective x-ray field across the adsorbate layer is expected to change at the substrate edge, particularly for grazing incidence. Detailed expressions for calculating such effects for PE from a uniform semi-infinite substrate (in the dielectric model) have been given elsewhere.[7,9,11] Here we have used a more general program due to Yang including all possible single and multiple reflections at any interfaces present, but still in the dielectric model.[26] Our XAS experimental results were used to derive the Ni dielectric constant via Kramers-Kronig analysis; the nonresonant constant for N_2 was taken from standard tabulations.[27] Figure 7 shows the N 1*s* intensities thus calculated for a monolayer of N_2 deposited on a 5-nm layer of Ni which is in turn deposited on a semi-infinite Ru crystal, at different incidence angles. For each range, a family of curves spanning the nominal value of the incidence angle is displayed. For the grazing-incidence case, Fig. 7(a) shows that there are significant modulations across the Ni $2p_{3/2}$ edge which strongly depend on photon energy and the angle of incidence. These modulations are approximately ±10% within ±2° of the nominal experimental angle and are brought about by rapid phase and amplitude variations of the x-ray wave in the surface region, including the superposition of wave components reflected from the vacuum-Ni and Ni/Ru interfaces. For the $2p_{1/2}$ threshold resonance above the $2p_{3/2}$ edge these variations are only roughly 1/3–1/5 as large.

In fact, the superposition of wave components arising from the two interfaces is expected to produce a set of peaks or dips in reflectivity in accordance with a Bragg-like relationship $n\lambda_{h\nu}=2d_{\mathrm{Ni}}\sin\theta_{h\nu,n}$, where $n=1,2,3,\ldots,\lambda_{h\nu}$ is the x-ray wavelength and d_{Ni} is the thickness of the Ni layer.[28] These features are often referred to as Kiessig fringes.[28] Calculations of reflectivity for our system of 3.1 Å N_2/50 Å Ni/semi-infinite Ru (not shown here) do indeed show such features. For example, at the Ni $2p_{3/2}$ resonance energy, minima of reflectivity are found at angles which are roughly multiples of 9° for our nominal layer thickness. However, for our specific choices of angles of incidence in the photoemission measurements, $\theta_{h\nu}=7°$, 40°, and 50°, the reflectivity is found to be close to that of a semi-infinite Ni layer. Furthermore, the actual layer thickness may deviate from the nominal thickness by +/− a few atomic layers, and it is likely that there is some variation of the thickness which will broaden the response. Therefore we do not expect these structures to play a major role in the

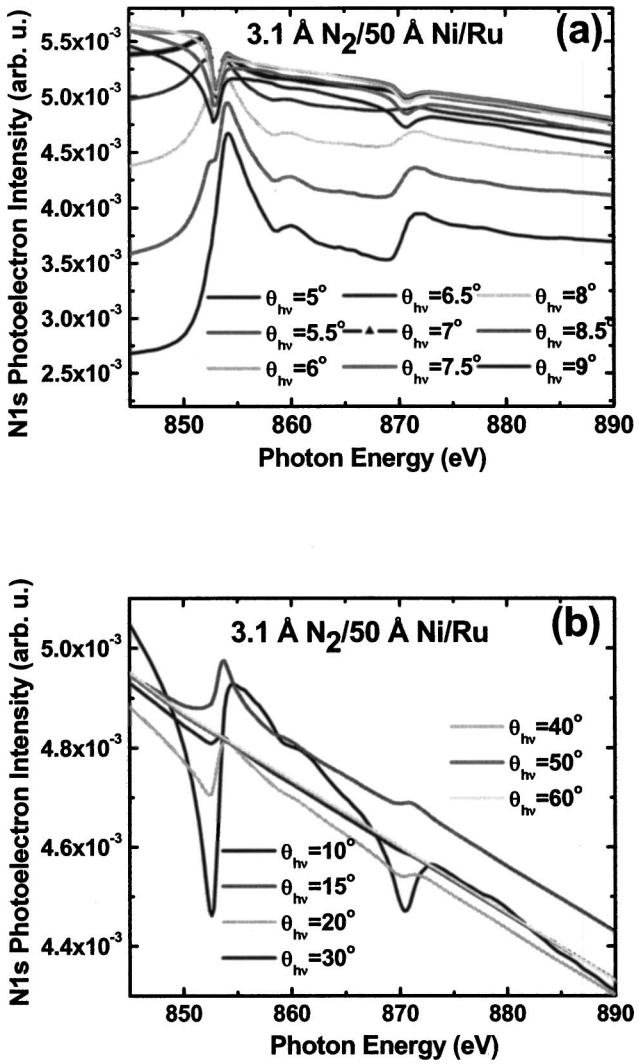

FIG. 7. Calculated modulations of the N 1*s* PE signal from a monolayer (0.3 nm) of N_2 on a 5-nm Ni film deposited on Ru, according to resonant x-ray optical (dielectric) theory (Refs. 7, 9, 11, and 26), as a function of photon energy in the Ni $2p_{3/2}$ range for various angles of photon incidence: (a) for grazing incidence angles, (b) for a wide range of angles including nongrazing incidence.

MARPE effects observed. In general, however, such Kiessig fringes need to be considered for any analysis of angle-dependent photoemission intensities from a nanometer-scale multilayer structure.

Comparing the experimental data in Figs. 2 and 5 to the dielectric x-ray optical calculations in Fig. 7(a), we conclude that for grazing incidence, straightforward x-ray optics will contribute considerably to the signal modulations found in both PE and PSD. We further note from these curves that the differences in the spectral shapes found in PE and PSD are most probably not significant because small errors in adjusting the angular orientation of the sample with respect to the photon beam suffice to explain them. In this connection we reiterate that, although XAS and PSD were measured simultaneously, so that exact energy *and* angle were identical, it was not possible to simultaneously measure PE and PSD. As Fig. 7(a) shows, the dielectric x-ray optical effects below the Ni $2p_{3/2}$ edge are a strong function of angle, largely due to reflection at the rear Ni/Ru interface; Fig. 5(a) bears this out for experiment. Inspection of the theoretical results shows that the field changes in front of the surface on a scale of 0.2 nm are very small, which explains the identical effect seen in the change of PE for the two N atoms and associated with the field enhancement (Fig. 1).

The situation is totally different for steeper photon incidence, on which emphasis is put in the calculations shown in Fig. 7(b). Here, reflection of the x-ray wave at both the surface and the rear interface is negligible even at the substrate thresholds, and the variation of the N 1*s* intensity across the Ni $2p_{3/2}$ edges predicted by the dielectric theory is below 1% for angles beyond 40°. Thus, any effects seen in this angle range or higher might be due to effects that go beyond the dielectric model and might be more associated with short-range interatomic coupling. As shown in Sec. III, we cannot exclude such an effect of the order of at most 5%, but the data are also consistent with no effect at all.

We therefore conclude that our results for N 1*s* excitation at the Ni 2*p* thresholds in the adsorbate system N_2 on Ni(111) are consistent with MARPE effects such as those seen previously for MnO, CuO, and NiO and which are due to field enhancement describable in terms of a resonant x-ray optical or dielectric model. We can put an upper limit of at most 5% on any effects going beyond the dielectric model. Initial indications of much bigger effects in our data have been traced back to beam damage. This again illustrates the extreme sensitivity of MARPE-type measurements to different types of experimental artifacts which can only be eliminated by very careful and detailed experimentation.

V. SUMMARY

In summary, for well-defined adsorbed layers of N_2 on Ni(111) films, we have found responses which qualitatively look like Fano resonances at the Ni $2p_{3/2}$ edge, both in N 1*s* photoemission and in N^+ photodesorption. In the case of PE, these raw data have been found to be strongly influenced by radiation damage—i.e., by stimulated desorption (mostly as neutral N_2 molecules) due to the outgoing electrons (photo, Auger, secondary) created by the photons absorbed in the bulk; this leads to strong coverage changes during measurement across the Ni resonances. Since the yield of these several types of electrons created by photoabsorption changes drastically at the Ni $2p_{3/2}$ edge and since this also happens for both grazing and steep angles of light incidence, this effect unfortunately leads to signal variations which, without correction, would appear to be evidence of MARPE-like intensity variations beyond a description in terms of x-ray optics. For the PE measurements, the extent of the artifacts induced in this way has been shown via comparison to x-ray optical calculations to be at least 95% of the raw effect for steep angles of incidence (40°–50°); for grazing angles, it constitutes up to half the raw effect. The true effect remaining for grazing incidence can be well understood as the consequence of dielectric x-ray optics—i.e., the change of amplitude and phase of the electromagnetic radiation in the

region of the very strong Ni resonances as described by the long-range dielectric response. These changes influence the PE signal strength directly; for the case of the N^+ emission, the responsible effect is a corresponding change of the intensity of outgoing electrons (photoelectrons and Auger electrons; low-energy secondaries are less efficient), leading to a small increase of ion emission caused by XESD. Quantitative deviations of the theoretical curves from the experimental values for grazing incidence, as well as between PE and PSD, may be due to small angle errors of a few degrees and averaging over a range of thicknesses for the case of thin Ni layer, which are difficult to avoid in our setup. The possible range of an effect at steep angles (at most 5% of the raw effect), where the dielectric x-ray optical effect is close to zero, is in the range where present theory would predict a weak interatomic core hole coupling between the Ni 2*p* bound-to-bound excited states on the one side and the N 1*s* one-hole (PE) and multihole (PSD) electron states on the other. Thus, agreement between experiment and the present state of theory is obtained.

We might add that these conclusions could only be reached by very extensive and careful experimentation and exclusion of artifacts. In the latter respect, MARPE—and especially any strictly local manifestations of it—has again shown itself to be an effect which can easily be confused with other phenomena occurring as absorption edges are crossed.

ACKNOWLEDGMENTS

We thank Z. W. Gortel for valuable discussions and K. Eberle and R. Schneider of E20, as well as the staffs of HASYLAB/Hamburg, of BESSY/Berlin, and of ELETTRA/Trieste, for their help and support during the experiments. This work has been supported in part by the Deutsche Forschungsgemeinschaft through Grant No. SFB 338 and through Project Nos. Wu 207/1, Me266/21, and Me266/22; by the German-Israeli Foundation (GIF Project No. I-557-217.05/97); by a Max-Planck prize to D.M.; by the German Fonds der Chemischen Industrie; and by the Director, Office of Energy Research, Basic Energy Science, Materials Science Division, of the U.S. Department of Energy (Contract No. DE-AC03-76SF00098).

*Corresponding author. Also at Fritz-Haber-Institut of the MPG, Berlin/Germany and at TASC, Trieste, Italy.

†Present address: IBM Almaden Research Center, San Jose, CA 95120.

[1] M. O. Krause, T. A. Carlson, and A. Fahlman, Phys. Rev. A **30**, 1316 (1984).

[2] See, e.g., U. Fano and J. W. Cooper, Rev. Mod. Phys. **40**, 441 (1968), and references therein.

[3] See, e.g., C.-O. Almbladh and L. Hedin, in *Handbook on Synchrotron Radiation*, edited by E.-E. Koch (North-Holland, Amsterdam, 1983), Vol. 1B, p. 611.

[4] P. Citrin, Phys. Rev. Lett. **31**, 1164 (1973).

[5] A. W. Kay *et al.*, Science **281**, 679 (1998).

[6] A. W. Kay *et al.*, J. Electron Spectrosc. Relat. Phenom. **103**, 647 (1999).

[7] F. J. García de Abajo, C. S. Fadley, and M. A. Van Hove, Phys. Rev. Lett. **82**, 4126 (1999).

[8] C. S. Fadley *et al.*, in *X-ray and Inner Shell Processes*, edited by R. W. Dunford *et al.*, AIP Conf. Proc. No. 506 (AIP, New York, 2000), p. 251.

[9] A. W. Kay *et al.*, Phys. Rev. B **63**, 115119 (2001); more details on detector nonlinearity correction appear in A. W. Kay, Ph.D. thesis, University of California, Davis, 2000.

[10] A. W. Kay *et al.*, J. Electron Spectrosc. Relat. Phenom. **114**, 1179 (2001).

[11] C. S. Fadley, in *Solid-State Photoemision and Related Methods: Theory and Experiment*, edited by W. Schattke and M. A. Van Hove (Wiley-VCH Verlag, Berlin, 2003), Chap. X.

[12] A. Kikas, E. Nõmmiste, R. Ruus, A. Saar, and I. Martinson, Solid State Commun. **115**, 275 (2000).

[13] A. Föhlisch *et al.* (unpublished).

[14] D. Nordlund *et al.*, Phys. Rev. B **63**, 121402(R) (2001).

[15] M. Finazzi *et al.*, Phys. Rev. B **62**, R16 215 (2000).

[16] N. Mannella *et al.* (unpublished results), available in preliminary form at: http://www-als.lbl.gov/als/compendium/AbstractManager/uploads/ACFCD.pdf

[17] E. Arenholz *et al.*, Phys. Rev. B **61**, 7183 (2000).

[18] A. Moewes, E. Z. Kurmaev, D. L. Ederer, and T. A. Callcott, Phys. Rev. B **62**, 15 427 (2000).

[19] J. Yoshinobu, R. Zenobi, Jiazhan Xu, Zhi Xu, and J. T. Yates, J. Chem. Phys. **95**, 9393 (1991); M. Ecker, Diploma thesis, Technical University Muenchen, 2001.

[20] P. Feulner *et al.*, Surf. Sci. **451**, 41 (2000).

[21] R. Weimar *et al.*, Surf. Sci. **451**, 124 (2000).

[22] P. Feulner *et al.*, Surf. Rev. Lett. **9**, 759 (2002).

[23] J. A. Meyer, P. Schmid, and R. J. Behm, Phys. Rev. Lett. **74**, 3864 (1995).

[24] R. Romberg *et al.*, Surf. Sci. **451**, 116 (2000).

[25] R. Weimar *et al.* (unpublished).

[26] S.-H Yang *et al.*, Surf. Sci. Lett. **461**, L557 (2000); S.-H. Yang *et al.*, J. Phys.: Condens. Matter **14**, L407 (2002).

[27] J. Yeh and I. Lindau, At. Data Nucl. Data Tables **32**, 1 (1985).

[28] See, for example, S. I. Khartsev, P. Johnsson, and A. M. Grishin, J. Appl. Phys. **87**, 2394 (2000).